ADVANCED MATERIALS TECHNOLOGIES
www.advmattechnol.de

Patterned, Wearable UV Indicators from Electrospun Photochromic Fibers and Yarns

*Yue Zheng, Weerapha Panatdasirisuk, Jiaqi Liu, Aijun Tong, Yu Xiang, and Shu Yang**

Wearable sensors allow for continuous and real-time monitoring of the human health and potential environmental hazards such as ultraviolet (UV) radiation on the daily basis. Here, textile-based wearable UV indicators are fabricated, which can show easily recognizable color patterns depending on UV irradiation intensity over time. The sensors are prepared by templating electrospun polycaprolactone fibers doped with photochromic dyes or embroidering the photochromic core–sheath yarns into commercial fabrics. This study provides a new design concept in developing smart wearable indicators.

1. Introduction

Wearable electronic products, including smart watches, smart glasses, and health monitoring bands, have entered our daily life. Many of them have begun to be incorporated into clothing as health monitors, batteries and supercapacitors, implants, or accessories.[1–8] While many wearable sensors have been developed,[7,9–11] most of them are thin film-based and worn directly on skin, which could be irritating over time. Therefore, there are increasing interests to create smart fabrics by integration of new functionalities into existing fabric materials through advanced manufacturing techniques. In particular, the use of environmentally responsive materials to create textile-based devices with recognizable patterns potentially will offer new platforms to embed intelligence for sensing, communication, monitoring, and data collection.

Among different wearable sensors, a few of them are passive ultraviolet (UV) indicators. Excessive exposure of UV radiation to our body over an extended period of time will not only generate wrinkles, but cause skin cancers. UV radiation from the sunlight, mainly UVA (320–400 nm) and UVB (280–320 nm), damages elastin, a protein in connective tissue.[12–14] UVA is linked to long term skin cell damages by aging and darkening the skin, while UVB causes skin burning and photokeratitis. Once elastin is broken down, the skin begins to lose its ability to recover to the original shape. Further, sun damage could be cumulative as it will gradually show the sign as we age. Therefore, UV index, an international standard to measure the strength of sunburn-producing UV radiation is developed by the World Health Organization (WHO) to monitor UV irradiation in real time outdoors.[15,16] UV index is calculated as the total UV radiation strength (mW m^{-2}) divided by 25 mW m^{-2} to get a constant value, typically between 0 and 15. The highest UV index ever recorded in a natural environment is 20. Generally, UV index above 6 indicates high risk of sunburn. A UV index above 11 is extremely dangerous. Humans should take all precautions or the unprotected skin and eyes can burn in minutes. To keep abreast of the UV index in the outdoor environment, a smart wearable sensor that can passively monitor UV index in real-time with high sensitivity will be highly desired.

Wearable UV detectors based on photocatalytic materials (e.g., TiO_2) to produce photocurrent under UV irradiation have been reported in films or meshes.[17,18] However, many have low sensitivity to sunlight and/or require use on external electronic devices (such as a smart phone) to display the detected data.[19–21] Compared to films, nano- and microfibers offer much larger surface area-to-volume ratio that could dramatically increase sensitivity, e.g., via multireflection of the sunlight on a meshed surface (see **Figure 1**a). Meanwhile, textile-based wearable sensors will offer benefits of flexibility, breathability, comfort, and conformability to body in addition to high sensitivity compared to film-based wearable sensors.[22–24] To create textile-based sensors, it will be essential to design and synthesize new functional materials that can be fabricated into fibers and yarns such that we can take advantage of existing knowledge in textile manufacturing, including weaving, knitting, embroidering, and nonwoven techniques.

UV-responsive fibers have been reported by doping organic photochromic dyes into polymer solution for electrospinning to demonstrate photoswitchability and applications for UV index indication.[25–29] Commercial UV sensing garments have been manufactured based on these fibers for atheistic effect, where color changes to different degrees under different UV strength. However, none has attempted to pattern the photochromic fibers or yarns for image recognition purpose. Simply changing color or varying the degree of color change by, for example, tuning the UV intensity and pH values, is not intuitive nor very accurate,

Y. Zheng, Dr. W. Panatdasirisuk, J. Liu, Prof. S. Yang
Department of Materials Science and Engineering
University of Pennsylvania
3231 Walnut Street, Philadelphia, PA 19104, USA
E-mail: shuyang@seas.upenn.edu
Y. Zheng, Prof. A. Tong, Prof. Y. Xiang
Department of Chemistry
Beijing Key Laboratory for Microanalytical Methods and Instrumentation
Key Laboratory of Bioorganic Phosphorus Chemistry
and Chemical Biology
Tsinghua University
Beijing 100084, P. R. China
The ORCID identification number(s) for the author(s) of this article can be found under https://doi.org/10.1002/admt.202000564.

DOI: 10.1002/admt.202000564

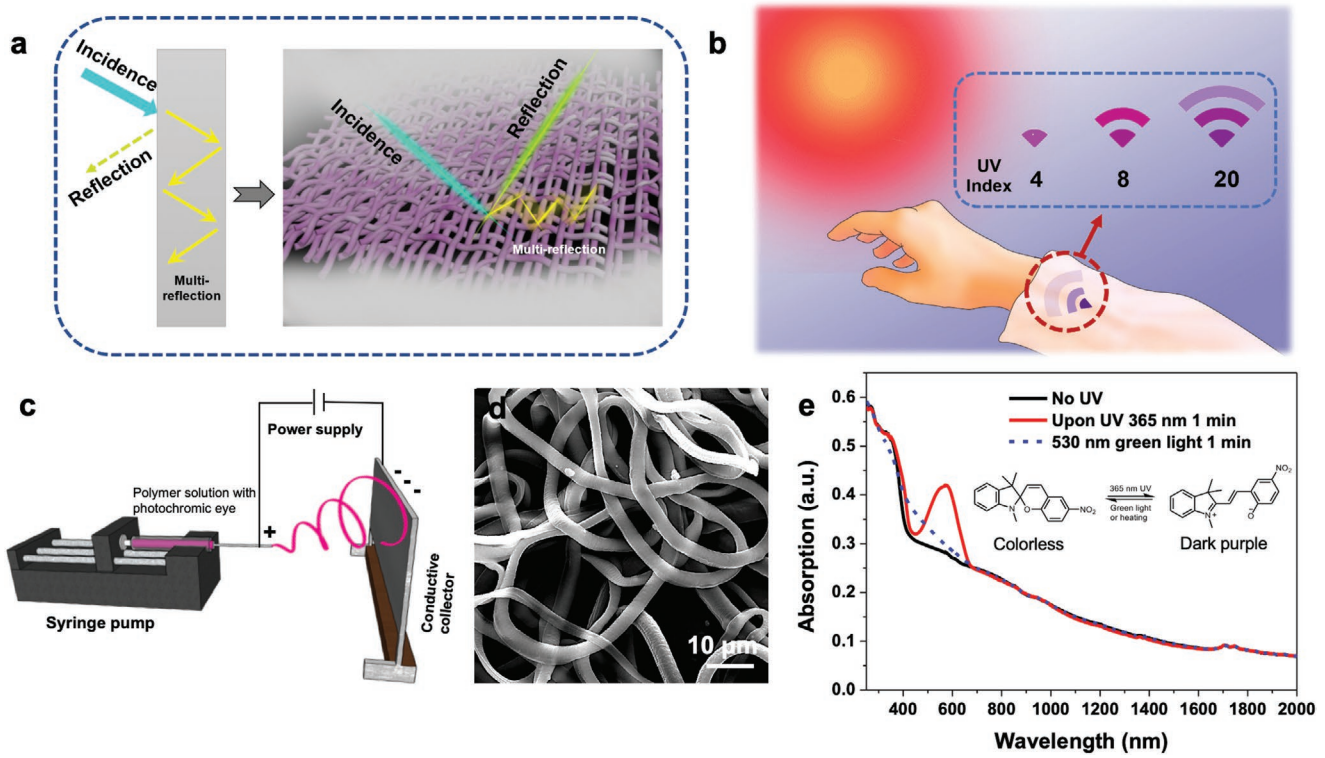

Figure 1. a) Illustration of multireflection on a fiber mesh, enabling good color contrast. b) Schematic illustration of the working mechanism of a patterned wearable UV sensor under sunlight. c) Schematic illustration of electrospinning process for fabrication of the PCL fiber mesh. d) Scanning electron microscopy (SEM) image of PCL nanofibers. e) Absorption spectrum of fiber mesh before and after specific light irradiation (dye percentage: 0.5 wt%: PCL); inset: photochromic mechanism of spiropyran.

especially when the concentration of analyte is very low. An intuitively recognizable pattern will offer advantages in indication, recognition, and information transmission. The ability of recognize color patterns and their changes will also offer potentials of using machine learning to recognize the patterns, classify data (here, UV intensity), and extract information from patterns even at a very low threshold. In turn, it will offer new opportunities to embed intelligence and communicate the results.[30]

Herein, we create photochromic fibers and yarns by electrospinning of polycaprolactone (PCL) doped with photochromic dyes for UV sensing, followed by proof-of-principle patterning. First, we electrospin photochromic fibers into different forms, including artificial tattoos, artificial leaves, and a Wi-Fi icon, to demonstrate the high UV sensitivity, and the possibility of patterning the fibers to differentiate UV exposure intensity (Figure 1b). We then create core (linen)–sheath (photochromic PCL) yarns, which have both high tensile strength and stretchability. When doped with UV- and pH-responsive dyes into PCL, respectively, we embroidered a grape pattern onto a linen fabric, which can turn into purple grapes and green leaves to demonstrate potential applications for multiresponsiveness recognition.

2. Electrospinning Photochromic Fiber and Nonwoven Meshes

Electrospinning (see setup in Figure 1c) offers a simple and high yield method to create nonwoven fibers with diameter ranging from 10 nm to 10 μm by jetting a charged polymer solution under a high electric field.[31] When jetted, the polymer solution is elongated and solidified before it lays itself randomly on a conductive collector. The motion for the jet and the final fiber size and morphology is a function of material properties, including conductivity, dielectric permittivity, dynamic viscosity, density, concentration and surface tension of the polymer solution, boiling point of the solvent, polymer molecular weight (MW), as well as operating conditions, including flow rate, applied electric field, and electric current.[32] Among various polymers that are electrospinnable, PCL is stretchable and relatively hydrophobic.[33,34] We have recently prepared PCL membranes by electrospinning for oil–water separation.[35] PCL fibers with an average diameter of 2.8 μm (see Figure 1d) show a stress-at-break of 6.59 ± 1.67 MPa with a strain up to 130 ± 21% without fracture. Importantly, for UV sensing applications, PCL has weak polarity, which will stabilize the photochromic dye, here, 1,3,3-trimethylindolino-6′-nitrobenzopyrylospiran (see Figure 1e), a type of spiropyran (SP). SP is colorless in its equilibrium state, therefore, offering good color change contrast upon UV irradiation. It undergoes reversible ring opening and close upon exposure to UV light (365 nm) and green light (530 nm), transforming the colorless dye into its color emitting merocyanin-form, showing the dark purple color (see Figure 1e). The equilibrium of the transformation is highly dependent on the polarity of the solvent. In a nonpolar solvent (e.g., toluene), the quantum yield of ring opening (Φ_o) and close (Φ_c) is on the same order of magnitude. [36] Therefore, the

degree of color change reflects the ratio of UV and green light intensity under sunlight.

It is noted that PCL has a relatively low glass transition temperature (T_g),[37] ≈60 °C. Thus, it will be best to fabricate and use PCL at room temperature or no greater than body temperature. This is important because photochromic dyes are sensitive to temperature, as they can be bleached at a higher temperature. Meanwhile, photochromic behaviors of spiropyran in PCL thin films has been studied.[38] Nonwoven meshes from spiropyran dye-doped PCL nanofibers has been reported, suggesting their suitability in textile applications due to their hydrophilicity and good washing fastness.[39] Simple patterns have been demonstrated by UV irradiation of the fiber mesh through a photomask. Nevertheless, the pattern is temporary and requires use of a photomask since the mesh itself is not patterned.

We first prepared PCL solution (14 wt%) in a mixed solvent[40] (methanol:dichloromethane (DCM) 3:7 v/v) consisting of 2 g L^{-1} sodium chloride to prepare uniform-sized fibers by electrospinning (see details in the Experimental Section). Different amounts of SP were added to the PCL solution for electrospinning (see Figure 1c). The polymer jet was collected on a conductive substrate, e.g., aluminum (Al) foil and copper wires. After solvent evaporation, the nonwoven SP/PCL fiber mesh was obtained. Depending on the shape of the conductive substrate, we could create patterned fiber mesh.

UV–vis–NIR absorption spectra of a nonwoven PCL fiber mesh consisting of 0.5 wt% SP dye (Figure 1e) showed that after UV irradiation at 365 nm for 1 min, an absorption peak appeared at λ_{max} = 581 nm, corresponding to dark purple color. When exposed to a green light at 530 nm for 1 min, the absorption peak at 581 nm disappeared. This process could be repeated at least 20 cycles (Figure S1, Supporting Information). Over time, the absorption peak at 581 nm gradually decreased due to photobleaching of the dye.

3. Fabrication of UV-Responsive Artificial Tattoos

To test the potential application of the SP/PCL fiber mesh as a wearable UV sensor, we first fabricated a temporary artificial tattoo from SP/PCL (see fabrication steps shown in **Figure 2**a). Similar to a commercial artificial tattoo, we used common printing paper after soaked in silicone oil as a waterproof backing paper, coated polyvinyl alcohol (PVA) thin film as an adherent water soluble sacrificial layer to release the coating, and commonly used organic surface adherents, propylene

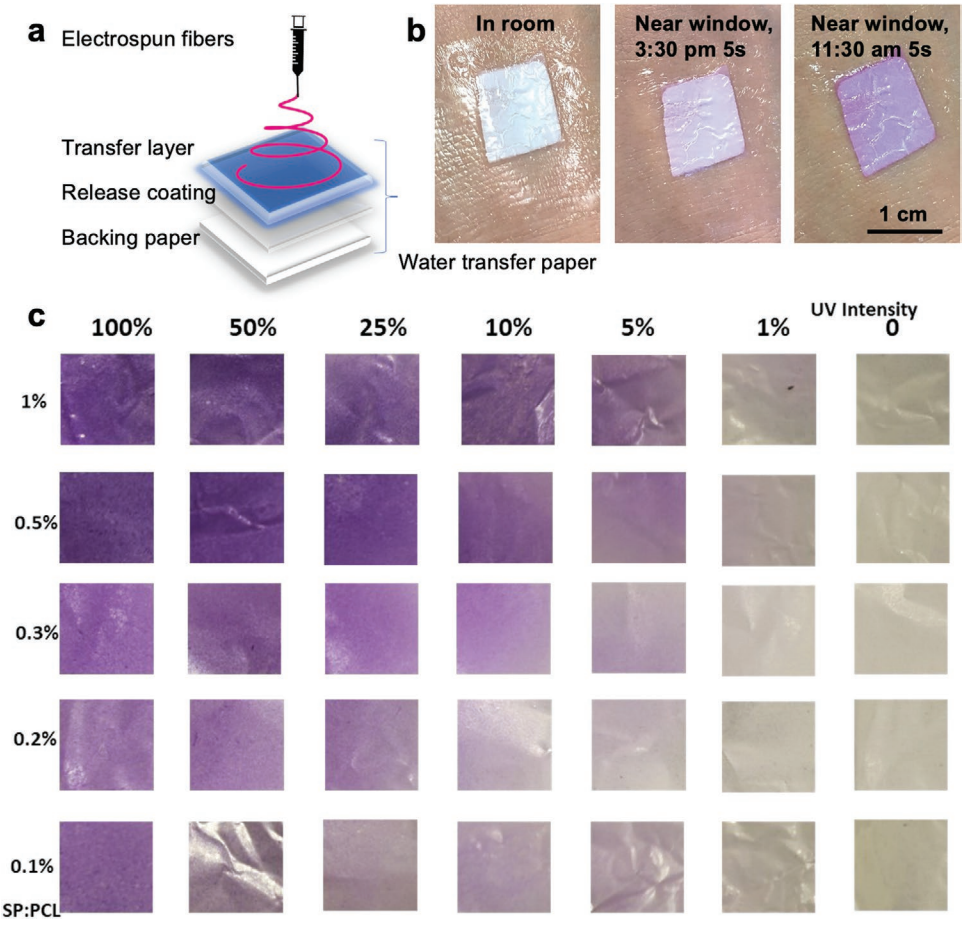

Figure 2. a) Schematic of the fabrication steps to create a temporary artificial tattoo. b) Photos of the SP/PCL fiber mesh tattoo placed on back of the hand under the indoor ambient lighting (left), near window at 3:30 pm for 5 s (middle), and near window at 11:30 am for 5 s (right) in mid-February. SP loading: 0.5 wt% of PCL. c) Degree of color change of the fiber mesh as a function of UV intensity and SP loading (0.1–1 wt% of PCL).

glycol methyl ether acetate (PGMEA), as a transfer layer for pattern printing. The fabricated artificial tattoo can be easily transferred to skin after wet by water and be peeled off. In our tests, the tattoo could remain firmly attached onto the skin for more than 24 h.

To test its ability to detect UV intensity under normal wear, we exposed the artificial tattoo to sunlight at different hours during the day. The original electropsun mesh appeared white under an indoor ambient lighting (see Figure 2b) due to random scattering of the PCL fibers. However, when moving hand with the tattoo to near window at 11:30 am and 3:30 pm (in mid-February), respectively, the mesh quickly turned to purple within 5 s with the one exposed at 11:30 am appeared darker, indicating UV index was higher near noon time.

To quantify the degree of color change as a function UV intensity and the loading of SP, we prepared PCL fiber mesh samples with different dye loadings (0.1–1 wt% SP vs PCL), and results are shown in Figure 2c. As expected, a higher SP loading and stronger UV intensity would deepen the purple color. Below 0.5 wt% SP, the degree of color change increased with the loading of SP; beyond 0.5 wt%, color change became saturated after UV irradiation reached beyond 25% of the maximum intensity used to change color of 0.1 wt% SP/PCL. Furthermore, our fiber mesh-based UV sensor can change color in response to UV intensity as low as 2 μW cm^{-2} (1% of the maximum intensity), the lowest threshold that the photocurrent-based UV sensors can achieve nowadays.[41] In fact, a UV index below 4 (10 μW cm^{-2}, 5% of the maximum intensity) in ambient conditions is completely safe to human and environmental UV intensity is typically not lower than 5 μW cm^{-2}. Clearly, our UV sensor performs well with distinguishable color changes within this range.

To check the efficacy of UV light sensing using an electropsun fiber mesh, we compared color change contrast from fiber mesh versus the spin coated thin film with the same dimension (width, w = length, l = 2 cm, and thickness, h = 10 μm) and loaded with the same amount of SP (0.5 wt%) in PCL (see Figure S2 in the Supporting Information). A significant color change is observed from the fiber mesh than that from a thin film, suggesting the actual dye concentration is different in these two forms of fiber-based UV sensors. We characterized SP loading by extracting SP first, followed by measurement using UV–vis spectra. The results showed that to achieve the same UV absorption value, SP loading (mol m^{-3}) in the thin film was nearly 4.5 times more than that in the fiber mesh (see the measurement and calculation details of actual spiropyran concentration in the Experimental Section). That is reasonable because fiber mesh is much more porous than the film, thus, has much larger surface area per volume to load more dyes. Together with multiscattering of light from the mesh surface, fiber-based materials will be more suitable for photochromic sensing to achieve high contrast at a low dye loading.

4. Templating Electrospun Fibers into Colored Patterns

The performance of a colorimetric sensor is dependent on several factors, including the color contrast, spatial frequency, and color content. Here, we first attempted to create color patterns by electrospinning SP/PCL fibers on a patterned conductive collector made of copper wire. As shown in **Figure 3**a, a centimeter-sized conductive "leaf" wired from copper was used as the conductive collector, which was connected to a power supply with a negative output voltage. Since negative charges were concentrated on the copper wire, electrospun SP/PCL fibers were drawn to the copper wire, forming a leaf with a simple midrib and secondary vein structures (Figure 3b). Due to multiscattering from the fiber surface, the as-spun "leaf" appeared white. Upon exposure to UV light (365 nm), the "leaf" gradually turned into vivid purple color only in the exposed regions, clearly showing the spatial localization of the photoresponse (Figure 3c). We then exposed the "leaf" to green (530 nm) light, SP dye turned transparent and the "leaf" was switched back to white. This process could be repeated many times. Nevertheless, the spacing between wires are rather large.

We then test the ability to create a leaf with a more complex venation pattern. To do so, we extracted the epicuticular wax, mesophyll, and other vascular tissues from an ivy leaf using a hot alkaline solution, leaving only the vein skeleton to sputter coat metal and created a conductive template for electrospinning SP/PCL (Figure 3d,e). As seen in Figure 3e, the tertiary and quaternary veins remained clearly seen from the electrospun leaf, demonstrating the ability to locally deposit the SP/PCL fibers on the metal coated vein regions.

We further created an artificial tattoo-based from the leaf venation vein pattern and applied it to the back of the hand. As seen from Figure S3 in the Supporting Information, despite the large size (≈6 cm^2), the leaf vein pattern can be conformally attached to the back of the hand. During the process of wearing more than 5 h, the tattoo remained to be firmly attached on hand. After peeling off, the vein pattern appeared intact, confirming the excellent conformability to hand and mechanical integrity of the tattoo. In contrast, a natural ivy leaf cannot be conformal to the hand.

Encouraged by the results, we then created a "Wi-Fi" icon with each radar beam made of electrospun PCL fibers, but consisting of different SP concentrations, 0.1, 0.25, and 0.5 wt%, respectively (Figure 3f). The gradual change of color of the beams would indicate the level of UV intensity, mimicking the "Wi-Fi" icon, where the flashing of the beams indicates the strength of the internet connection. As Figure 3g shows, When UV intensity was at the lowest (UV index = 4), the bottom beam turned purple. When UV index turned 12, the bottom and middle beams turned purple. When UV index was at the highest, 20, all three beams turned purple, suggesting that people should take measures to protect themselves from potential UV damage.

5. Embroidery of Photochromic Yarns on an Existing Fabric

Compare to films or artificial tattoos, textile-based wearable sensors will offer additional benefits, such as comfort, breathability, and the ability to be integrated directly into an existing garment. To demonstrate the potential to create a UV-responsive textile, here, we twisted PCL fibers into yarns, which can be woven, sewn, or embroidered on an existing fabric

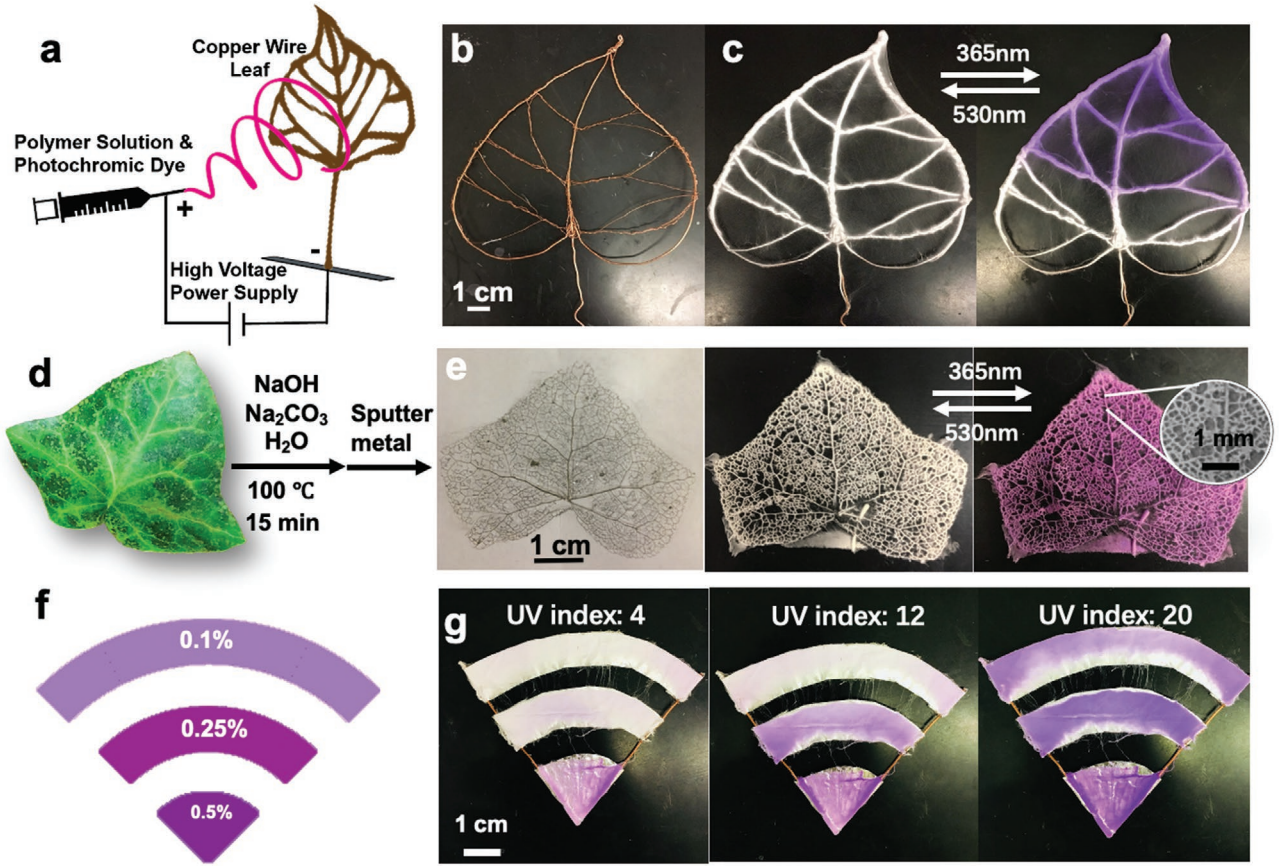

Figure 3. a) Schematic of the electrospinning setup for fabrication of leaf-shaped nanofiber mesh. Photos of b) a copper wire "leaf," and c) after coating of SP/PCL fibers, which can change colors reversibly depending on the exposed wavelength of light. Photos of d) an ivy leaf, and e) the corresponding skeleton after NaOH etching and metal sputtering, which could change colors. f) Illustration of a "Wi-Fi" icon changing color to different degrees, corresponding to different SP concentrations in each beam. g) Photo of the "Wi-Fi icon made from electrospun SP/PCL fibers under UV irradiation (UV index of 4, 12, and 20, respectively) for 5 s.

(**Figure 4**a). As seen from Figure S4 in the Supporting Information, two syringes connected to power supplies of opposite sign of voltage jetted out the polymer fibers, which were attracted to the rotating metal funnel and twisted into a yarn that is then pulled out and collected on a rotating drum continuously, up to 25 m long. A single PCL yarn, however, is not strong enough to endure significant mechanical stretching or pulling, especially on a commercial knitting/weaving machine. As a proof-of-concept, to enhance the mechanical strength of the yarn and to better show the color change on the yarn, we created a core–sheath yarn where the commercial linen is used as the core yarn and electrospun SP/PCL fibers would wrap around the core yarn to form the sheath (see illustration in Figure 4b). Scanning electron microscopy (SEM) images confirmed the core–sheath structure of the fabricated yarns (Figure 4c). Linen is chosen as the core yarn because it has been widely used in textile for its high mechanical strength. However, it is not very stretchable. As seen in Figure S5 in the Supporting Information, the commercial linen yarn break when stretched over 2% strain, followed by a sharp drop in stress. In contrast, PCL has excellent stretchability,[35] which is important for the fabric to be conformal to the body. In our experiments, the pure PCL yarn could be stretched more than 400% strain. By combining the two materials system into one, we could not only increase the tensile strength but also maintain the stretchability to some degree. As seen in Figure S5 in the Supporting Information, the core (linen)–sheath (photochromic PCL) yarn reached the maximum stress at ≈4% strain. Interestingly, afterward, the stress dropped gradually unlike the pure linen, presumably the PCL sheath kept the linen core from complete failure, until reaching 9% strain. The colorimetric property was maintained in the fabricated core–sheath yarns. As seen in Figure 4d, the core–sheath yarn changed color reversibly, from white to purple under 365 nm light irradiation and returned back to white after 530 nm exposure for a few minutes.

Lastly, we embroidered a grape pattern from the core–sheath yarn on a linen fabric. As PCL sheath is very thin and flexible, the core–sheath yarn is comfort and stable like the commercial linen yarn without any delamination of the core or sheath in our hands during the embroidery process. As Figure 4e shows, after 365 nm UV irradiation (at UV index ≈15), the purple grapes emerged on the undyed linen fabric, which appeared as neutral taupe with grey undertone, indicating that UV intensity in the environment is strong at that time. For environmental sensors, the multiparameter sensing in response to different stimuli in the ambient environment is far more attractive in practical applications yet it remains challenging to fabricate such kind of sensors with high selectivity.[42] Here, we attempted to create a

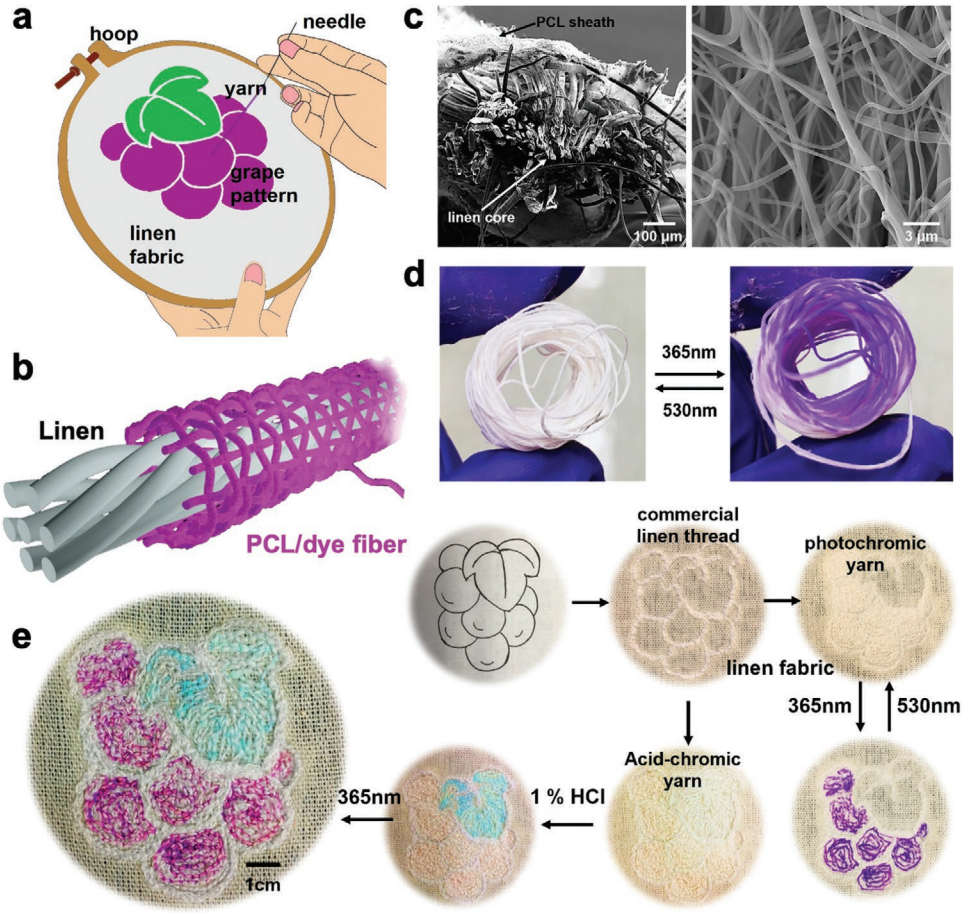

Figure 4. An embroidered grape pattern that is both UV- and pH-responsive. a) Illustration of embroidery of a grape pattern. b) Illustration of a linen core–PCL sheath yarn. c) SEM images of the core–sheath yarn: cross-sectional view (left) and side view (right). d) Photographs of the core–sheath yarn upon exposure to light of different wavelengths, 365 nm (right) and 530 nm (left). e) The UV and pH responsiveness of a grape pattern embroidered on a commercial linen fabric.

dual-responsive sensor by adding pH responsiveness. To do so, we added pH-responsive triphenylmethane dye, malachite green, which turned from colorless to green when the pH value is above 1.8 (see color change mechanism in Figure S6 in the Supporting Information), in PCL to create a pH-responsive yarn that could be embroidered into a grape leaf to detect the environmental acidity, which is another indicator of the environmental hazard. As seen in Figure 4e, the leaf pattern turned green when exposed to 1 wt% HCl aq. solution. The color green and purple can be activated separately or simultaneously. We note that the embroidered fabric can be sewed onto any other fabrics to be worn by the users.

6. Conclusion

In conclusion, we electrospun color changing polymer fibers and twisted them into yarns and demonstrated their uses as wearable UV sensors in different easily recognizable patterns, including a leaf with vascular structures, a Wi-Fi icon, and embroidered grapes. The photochromic dye (spiropyran)-doped PCL nanofibers showed high sensitivity and quick response to UV light, turning colorless fibers into purple under the natural sunlight. The color change contrast appeared greater than that from a film, even at a much lower dye loading. By using pre-formed conductive wires as the collectors, the UV-responsive nonwoven fibers could be fabricated into different patterns for potential applications such as identification. A UV-responsive artificial tattoo was fabricated from the nonwoven fiber mesh, demonstrating superior conformability as wearable UV index sensors. The design of core–sheath yarn with linen yarn as the core coated with dye-doped PCL fibers as sheath showed significantly improved mechanical properties, allowing for embroidery the yarns into grapes with leaves onto a commercial linen fabric, demonstrating both UV and pH responsiveness. Our study presents the first example that combines environmentally responsive materials and textile fabrication into color patterned sensors. It opens the door for integration of machine learning and intelligence in smart fabrics.

7. Experimental Section

Materials: PCL (Mw ≈80 000), PVA (Mowiol 20-98, Mw ≈125 000), PGMEA (purity ≥99.5%), methanol (purity ≥99.5%), silicone oil (378356-

250 ML viscosity 50 cSt), sodium chloride (NaCl, purity ≥99.5%), sodium carbonate (Na_2CO_3, purity ≥99.0%), and malachite green carbonyl base (pH-responsive dye, purity >98%) were purchased from Sigma-Aldrich. 1,3,3-trimethylindolino-6′-nitrobenzopyrylospiran (photochromic dye, SP, purity >98%) was purchased from TCI America. All chemicals were used as received without further purification. Commercial linen thread (ASIN: B0795BWXFD) and water decal transfer paper (ASIN: B06XP7NZ62) were purchased from Amazon.com and used as received.

Characterization: SEM images were taken from FEI Quanta 600 environmental scanning electron microscopy (ESEM) at 15 kV. Photochromic experiments were performed using a 4-wavelength high-power LED source operated by a DC4104 driver from Thorlabs. UV intensity was measured by Newport Power Meter Model 1815-C. Tensile tests were performed on the INSTRON 5564 with a 100 N load cell at a speed of 2.5 mm min^{-1}. UV–vis spectra were obtained using the Agilent Cary 5000 spectrophotometer.

Electrospinning of Photochromic PCL Fiber Meshes: The PCL solution (14 wt%) for electrospinning was prepared in mixed solvents. In order to improve the conductivity of the polymer solution and obtain fine nanofibers, 2 g L^{-1} NaCl solution was mixed in methanol with DCM in a ratio of DCM:NaCl (MeOH)aq = 7:3 (v:v). Different amounts of SP solid powder were added into the PCL solution until it was well dissolved to prepare electrospinning solutions with different dye concentrations. The SP/PCL solution was electrospun at a flow rate of 0.01 mL min^{-1}, 12 kV onto an aluminum foil as the conductive collector. The distance from the tip of spinneret to the conductive collector was kept at 15 cm.

Fabrication of Photochromic Ivy Leaf Vein Patterns: 3.5 g NaOH, 2.5 g Na_2CO_3, and 100 mL water were mixed in a 200 mL beaker to prepare the etching solution to remove epicuticular wax, mesophyll, and other vascular tissues. The freshly picked ivy (*Hedera nepalensis var. sinensis* (Tobl.) Rehd) leaf was placed into the above solution and heated to 100 °C for 15 min, followed by washing the leaf in cold water to remove mesophyll. After the resulting leaf vein was let dry naturally, it was sputter coated with Au/Pd to obtain a conductive template for electrospinning.

Fabrication of the Wi-Fi Pattern: A Wi-Fi icon pattern was fabricated using the copper wire as support and aluminum foils that could be cut into Wi-Fi "beams" of different sizes. Copper wire was used to connect each "beam" such that the entire pattern was conductive. Finally, the aluminum foils were glued to the copper wire using a conductive paste.

Preparation and Application of UV-Responsive Temporary Artificial Tattoos: A standard A4 printing paper was soaked in silicone oil (as a release coating) for 1 h as the backing paper. After being dried, the treated paper was cut and paste on a petri dish. Then, 2 mL PVA solution (10 wt% in DI water) was poured on the paper and applied evenly. After the water was evaporated completely, the photochromic PCL thin film was laminated onto the PVA treated paper. The photochromic PCL thin film (10 µm thick) used in the artificial tattoo was prepared by spin coating 14 wt% PCL in PGMEA at 1500 rpm s^{-1} on the CEE200X spin coater from Brewer Science. Concentration of 1,3,3-trimethylindolino-6′-nitrobenzopyrylospiran was 0.5 wt% in PCL.

The entire package could be easily peeled off as the temporary artificial tattoo. To apply the tattoo to skin, the skin was first cleaned and moisturized. Then, the patterned side of the tattoo was applied to the skin, followed by wetting the backing paper with water. After slowly peeling off the backing paper, the UV-responsive artificial tattoo was successfully transferred to the skin.

Fabrication of an Embroidered Grape Pattern: Both photochromic and pH-responsive core–sheath yarns were fabricated using the device shown in Figure S4 in the Supporting Information. The linen thread was used as the core yarn and threaded through a metal funnel, while photochromic and pH-responsive PCL fibers were electrospun onto the core yarn as the sheath from two sets of syringe pumps with opposite charges, followed by twisting on a metal funnel. The yarn was taken away by a winder, allowing for continuous fabrication of the PCL yarn tens of meters long. PCL concentration was 14 wt% in the mixed solvent described before. SP concentration was 0.5 wt% of PCL. pH-responsive malachite green concentration was 1×10^{-3} M in DCM. The obtained core–sheath yarn was embroidered on a linen fabric with a grape pattern through the embroidery pinhole, where the pH-responsive yarn was embroidered as leaves and the photochromic yarn was embroidered to make the grapes.

Measurement of Actual SP Concentrations in the PCL Fiber Mesh and Film: To quantify the actual SP concentration in the PCL fiber mesh and films, samples with dimension of 2 cm (l) × 2 cm (w) × 10 µm (h) were cut in squared shapes with the same initial SP loading, 0.5 wt%, in the PCL solution, respectively. Each sample was soaked in 4 mL acetone overnight to extract SP from PCL. Then, the SP/acetone solution was filtered to remove undissolved PCL for UV absorption measurement at 350 nm. SP concentration in each sample can be calculated according to

$$\text{dye conc.} = \frac{c \times V_{sol}}{l \times w \times h} \tag{1}$$

where c is the concentration of each sample in acetone. Here, $V_{sol} = 4$ mL. The calculated SP concentrations were 39.69 and 184.0 mol m^{-3} in the PCL fiber mesh and thin film, respectively.

Supporting Information

Supporting Information is available from the Wiley Online Library or from the author.

Acknowledgements

The authors thank the financial support from Tsinghua University for support of student exchange. S.Y. acknowledges the partial support by the American Chemical Society (ACS) Petroleum Research Fund (PRF) grant, No. 573238. Yuchen Wang and Yuchong Gao are acknowledged for help in mechanical testing. Geneviève Dion (Drexel University) is acknowledged for helpful discussion.

Conflict of Interest

The authors declare no conflict of interest.

Keywords

core–sheath yarns, electrospinning, patterns, textile-based sensors, wearable ultraviolet sensors

Received: June 9, 2020
Revised: August 16, 2020
Published online: September 13, 2020

[1] X. A. Zhang, S. Yu, B. Xu, M. Li, Z. Peng, Y. Wang, S. Deng, X. Wu, Z. Wu, M. Ouyang, Y. Wang, *Science* **2019**, *363*, 619.
[2] W.-H. Yeo, Y.-S. Kim, J. Lee, A. Ameen, L. Shi, M. Li, S. Wang, R. Ma, S. H. Jin, Z. Kang, Y. Huang, J. A. Rogers, *Adv. Mater.* **2013**, *25*, 2773.
[3] Y. Li, Y. Li, M. Su, W. Li, Y. Li, H. Li, X. Qian, X. Zhang, F. Li, Y. Song, *Adv. Electron. Mater.* **2017**, *3*, 1700253.
[4] K. Jost, D. Stenger, C. R. Perez, J. K. McDonough, K. Lian, Y. Gogotsi, G. Dion, *Energy Environ. Sci.* **2013**, *6*, 2698.
[5] K. Jost, D. P. Durkin, L. M. Haverhals, E. K. Brown, M. Langenstein, H. C. De Long, P. C. Trulove, Y. Gogotsi, G. Dion, *Adv. Energy Mater.* **2015**, *5*, 1401286.
[6] K. Jost, G. Dion, Y. Gogotsi, *J. Mater. Chem. A* **2014**, *2*, 10776.

[7] P.-C. Hsu, A. Y. Song, P. B. Catrysse, C. Liu, Y. Peng, J. Xie, S. Fan, Y. Cui, *Science* **2016**, *353*, 1019.
[8] L. M. Castano, A. B. Flatau, *Smart Mater. Struct.* **2014**, *23*, 053001.
[9] D. Yu, Q. Qian, L. Wei, W. Jiang, K. Goh, J. Wei, J. Zhang, Y. Chen, *Chem. Soc. Rev.* **2015**, *44*, 647.
[10] D.-H. Kim, N. Lu, R. Ma, Y.-S. Kim, R.-H. Kim, S. Wang, J. Wu, S. M. Won, H. Tao, A. Islam, K. J. Yu, T.-I. Kim, R. Chowdhury, M. Ying, L. Xu, M. Li, H.-J. Chung, H. Keum, M. McCormick, P. Liu, Y.-W. Zhang, F. G. Omenetto, Y. Huang, T. Coleman, J. A. Rogers, *Science* **2011**, *333*, 838.
[11] W. Gao, S. Emaminejad, H. Y. Y. Nyein, S. Challa, K. Chen, A. Peck, H. M. Fahad, H. Ota, H. Shiraki, D. Kiriya, D.-H. Lien, G. A. Brooks, R. W. Davis, A. Javey, *Nature* **2016**, *529*, 509.
[12] F. R. de Gruijl, *Eur. J. Cancer* **1999**, *35*, 2003.
[13] D. E. Brash, J. A. Rudolph, J. A. Simon, A. Lin, G. J. McKenna, H. P. Baden, A. J. Halperin, J. Pontén, *Proc. Natl. Acad. Sci. USA* **1991**, *88*, 10124.
[14] R. B. Setlow, *Proc. Natl. Acad. Sci. USA* **1974**, *71*, 3363.
[15] V. Fioletov, J. B. Kerr, A. Fergusson, *Can. J. Public Health* **2010**, *101*, I5.
[16] Report of the WMO Meeting of Experts on UV-B Measurements, Data Quality and Standardization of UV Indices, (UV Monitoring and Assessment Program Panel, World Meteorological Organization (WMO), Global Atmosphere Watch, Global Environment Monitoring System), World Meteorological Organization, Geneva, Switzerland **1994**.
[17] X. Xu, J. Chen, S. Cai, Z. Long, Y. Zhang, L. Su, S. He, C. Tang, P. Liu, H. Peng, X. Fang, *Adv. Mater.* **2018**, *30*, 1803165.
[18] R. D. Schaller, V. M. Agranovich, V. I. Klimov, *Nat. Phys.* **2005**, *1*, 189.
[19] M. Qiu, P. Sun, Y. Liu, Q. Huang, C. Zhao, Z. Li, W. Mai, *Adv. Mater. Technol.* **2018**, *3*, 1700288.
[20] X. Xu, Y. Zuo, S. Cai, X. Tao, Z. Zhang, X. Zhou, S. He, X. Fang, H. Peng, *J. Mater. Chem. C* **2018**, *6*, 4866.
[21] A. J. Nozik, *Nat. Nanotechnol.* **2009**, *4*, 548.
[22] J. Eom, R. Jaisutti, H. Lee, W. Lee, J.-S. Heo, J.-Y. Lee, S. K. Park, Y.-H. Kim, *ACS Appl. Mater. Interfaces* **2017**, *9*, 10190.
[23] A. Chinnappan, C. Baskar, S. Baskar, G. Ratheesh, S. Ramakrishna, *J. Mater. Chem. C* **2017**, *5*, 12657.
[24] R. Paradiso, N. Taccini, G. Loriga, in *The Engineering Handbook of Smart Technology for Aging, Disability, and Independence* (Eds: A. Helal, M. Mokhtari, B. Abdulrazak), John Wiley & Sons, Hoboken, NJ **2008**, pp. 673–692.
[25] F. Di Benedetto, E. Mele, A. Camposeo, A. Athanassiou, R. Cingolani, D. Pisignano, *Adv. Mater.* **2008**, *20*, 314.
[26] A. A. Merati, in *Advanced Textile Engineering Materials* (Eds: S.-U. Islam, B. S. Butola), Scrinever Publishing, Beverly, MA **2018**, pp. 1–29.
[27] M. Parhizkar, Y. Zhao, T. Lin, in *Handbook of Smart Textiles* (Ed: X. Tao), Springer, Singapore **2014**, p. 1.
[28] A. P. Periyasamy, M. Vikova, M. Vik, *Text. Prog.* **2017**, *49*, 53.
[29] D. Sun, M. Chen, K. H. An, S. Clark, *Adv. Res. Text. Eng.* **2018**, *3*, 1030.
[30] Z. Zhang, L. Cui, X. Shi, X. Tian, D. Wang, C. Gu, E. Chen, X. Cheng, Y. Xu, Y. Hu, J. Zhang, L. Zhou, H. H. Fong, P. Ma, G. Jiang, X. Sun, B. Zhang, H. Peng, *Adv. Mater.* **2018**, *30*, 1800323.
[31] X. Wang, B. Ding, G. Sun, M. Wang, J. Yu, *Prog. Mater. Sci.* **2013**, *58*, 1173.
[32] Z.-M. Huang, Y. Z. Zhang, M. Kotaki, S. Ramakrishna, *Compos. Sci. Technol.* **2003**, *63*, 2223.
[33] M. F. Canbolat, A. Celebioglu, T. Uyar, *Colloids Surf., B* **2014**, *115*, 15.
[34] T. Potrč, S. Baumgartner, R. Roškar, O. Planinšek, Z. Lavrič, J. Kristl, P. Kocbek, *Eur. J. Pharm. Sci.* **2015**, *75*, 101.
[35] W. Panatdasirisuk, Z. Liao, T. Vongsetskul, S. Yang, *Langmuir* **2017**, *33*, 5872.
[36] A. K. Chibisov, H. Görner, *J. Phys. Chem. A* **1997**, *101*, 4305.
[37] B. Saad, U. W. Suter, in *Encyclopedia of Materials: Science and Technology* (Eds: K. H. J. Buschow, R. W. Cahn, M. C. Flemings, B. Ilschner, E. J. Kramer, S. Mahajan, P. Veyssière), Elsevier, Oxford **2001**, p. 551.
[38] A. Samoladas, D. Bikiaris, T. Zorba, K. M. Paraskevopoulos, A. Jannakoudakis, *Dyes Pigm.* **2008**, *76*, 386.
[39] S. Ali, F. Ahmed, Z. Khatri, S. H. Kim, *Text. Sci. Eng.* **2015**, *52*, 126.
[40] V. Beachley, X. Wen, *Mater. Sci. Eng., C* **2009**, *29*, 663.
[41] L. Suresh, J. V. Vaghasiya, D. K. Nandakumar, T. Wu, M. R. Jones, S. C. Tan, *Chem* **2019**, *5*, 1847.
[42] Y. Yang, Z. D. Deng, *Appl. Phys. Rev.* **2019**, *6*, 011309.